

Analysis of Design Flood Using Synthetic Unit Hydrograph Methods of Snyder and Soil Conservation Service in the Padang Watershed

Tri Aldi Notatema Zendrato¹, Ivan Indrawan^{1*}, Emma Patricia Bangun¹

¹Department of Civil Engineering, Faculty of Engineering, Universitas Sumatera Utara, Medan, 20155, Indonesia

*Corresponding Author: ivan.indrawan@usu.ac.id

ARTICLE INFO

Article history:

Received 20 November 2025

Revised 8 December 2025

Accepted 9 December 2025

Available online 12 December 2025

E-ISSN: -

P-ISSN: -

How to cite:

Zendrato, T. A., Indrawan I. and Bangun, E.P. "Analysis of Design Flood Using Synthetic Unit Hydrograph Methods of Snyder and Soil Conservation Service in the Padang Watershed", Journal of Civil Engineering and Public Infrastructure Management, vol. 01, no. 01, 2025.



This work is licensed under a Creative Commons Attribution-ShareAlike 4.0 International.

ABSTRACT

This research analyses the design flood discharge on the Padang River by using the Synthetic Unit Hydrograph (SUH) Snyder and SUH Soil Conservation Service (SCS) methods. The rainfall area calculation employs the Polygon Thiessen method while the rainfall intensity analysis implements the Mononobe method and the hourly rainfall distribution uses the Alternating Block Method (ABM). Based on the HSS Snyder method, the peak time lies in the 18th hour with the peak discharge being estimated at 583,10; 668,04; 769,53; 841,59 and 911,11 m³/s for each return period of 5-, 10-, 25-, 50- and 100-year. This peak time is larger yet its peak discharge is smaller than the estimations based on the HSS SCS method. The peak discharge is predicted as much as 1037,80; 1187,31; 1365,95; 1492,80 and 1615,17 m³/s for the return period of 5, 10, 25, 50 dan 100 year with its peak time lies in the 10th hour. Analysis of comparison between the predictions undertaken by the two different HSS methods suggests some practical considerations.

Keywords: *Design flood, Padang watershed, SCS, Snyder, Synthetic Unit Hydrograph*

1. Introduction

Urban flood may arise due to water overspilling from a dam into a river or as a result of the exceeded capacity of a water body such as a lake or river [1]. Water overflowing from the Padang river had frequently caused flooding in the major areas of Tebing district mainly due to the change in the land use and the development causing destructions in the riverbank area. This caused significant economic loss among the local societies due to the destructions in the public facilities, private houses and agricultural land. The BPBD Sumatera Utara confirmed that four subdistricts, namely Padang Hulu, Padang Hilir, Rambutan and Bajen, were reportedly flooded in November 2020 [2]. An observation taken on the 28 November 2020 confirmed that there had been 25.297 people affected by the flood, significant destructions in the embankments and economic loss worth up to 50 million rupiah [2]. A more recent flooding disaster that occurred in November 2025 has impacted 6.971 houses and 24.332 people [3]. These series of event indicate that the areas in the Tebing district are vulnerable to flooding disaster.

One of the strategies to mitigate flood is by setting up a water management structure in problematic areas. The design of such a structure typically requires design flood discharge. This is based on the understanding that an accurate mitigation planning including assessing the flood discharge will reduce the risk of construction failure

associated with the flood disaster [4]. Therefore, an important step prior to designing the water management structure is predicting accurately the design flood discharge.

One approach to predict the design flood discharge is by employing a hydrograph-based method and adopting actual rainfall data recorded at credible and representative rainfall stations [5]. This method allows hydrologists to estimate variation of flood discharge with time. Prediction of design flood discharge and hence planning of flood disaster control require such a hydrograph curve that is relevant to the actual condition of the watershed under investigation [4]. In order to generate the representative hydrograph of a watershed, measurements of historical data need to be undertaken through Automatic Water Level Recorder (AWLR) at the relevant water gauge stations. This generates data of flow discharge, daily rainfall and hourly rainfall and its variation with time [6]. Such on-site measurements, however, are not always accessible due to many reasons. As a result, the availability of water-level time series may either be very limited or not accessible publicly. When measurement of flood discharge is rarely done or even has never been carried out, the hydrograph is analysed using a Synthetic Unit Hydrograph (SUH) method. This approach considers the characteristic of the watershed. Nevertheless, using this approach requires modification and calibration to calculate the peak discharge and the curve of hydrograph that correspond to the existing data [4].

To tackle the problem associated with the limited data, a SUH Snyder method has been developed and the unit hydrograph may be derived using this method [6]. The concept of this SUH Snyder method was proposed in 1938 by F.F. Snyder of the United States. This method considers some parameters associated with the watershed to obtain the hydrograph and has derived the values of two physical parameters namely the slope coefficient and the storage capacity coefficient based on the topographical condition of the Appalachian highlands [6]. Estimations of its watershed area are given in a range of 30 to 30.000 km² [7]. Given the empirically inherent parameters, it may be necessary to adjust the parameter values following the actual topographical condition of a watershed. The two parameters may depend on the characteristics of the watershed under interest.

Another method based on the SUH is referred to as Soil Conservation Service (SCS). This dimensionless unit hydrograph is a method to obtain the hydrograph curve of a watershed for which limited or no actual data of flow discharge is available [6]. This indicates that the synthetic unit hydrograph can be derived by employing time and discharge comparisons for the watershed being investigated. Victor Mockus of the USA has developed the SUH SCS method in 1972 [8]. The associated parameters cover time abscission and discharge ordinate. Essentially, the first refers to a comparison between time and peak time while the latter indicates a comparison between the discharge and the peak discharge. The SUH SCS employs curve number values that describe how land use and land cover of the watershed impact the runoff flow over the ground surface. These curve number values determine the conversion of the rainfall data into the runoff flow discharge arising in the watershed [6]. Earlier studies undertaken by Erwanto and Barried [9] have confirmed that a hydrograph modelling of the Tambong Banyuwangi watershed can be implemented to indicate whether the watershed has a potential land use. The hydrological parameter values were evaluated through modelling the area based on the HSS SCS and application of Hydrologic Engineering Center (HEC)-Hydrologic Modelling System (HMS). Furthermore, the analysis has confirmed the impact of the land use on the effectiveness of watershed management.

Given the importance of predicting the design flood discharge and the frequent occurrence of flooding in the area around the Padang watershed, the present study aims to evaluate the design flood discharge. An earlier study has adopted conventional, non-hydrographic based methods including the Mean Annual Flood, Melchior and the Haspers method to evaluate this discharge [10]. However, these methods lack of information regarding the variation of the discharge with time and hence the peak time and the peak discharge. The present study adopts a hydrograph approach for analysing the hydrograph characteristics of the watershed and its dependence on return period. This study also seeks to understand the comparisons generated from the SUH Snyder and the SUH SCS. By confirming the comparisons, the importance of empirical coefficients and parameters used in the SUH Snyder will be identified.

2. Method

This research study is concerned with the Padang watershed located in the province of North Sumatera. The watershed stretches over the regency of Simalungun, Serdang Bedagai and the district of Tebing Tinggi. Geographically, the main river has a length of 60,52 km and covers an area of 1108,31 km² [11]. Data required for the present investigation includes maximum daily rainfall measured over a span of ten years (2012-2021) at different rainfall stations. This data was obtained from the First Class of Sampali, the Indonesian Agency for Meteorological, Climatological and Geophysics. Furthermore, the topographic map, the soil classification and the land cover map representing the Padang watershed were utilized to undertake this study.

The average of rainfall was predicted using the Polygon Thiessen method based on Equation (1) [12].

$$\bar{R} = \frac{A_1 R_1 + A_2 R_2 + A_3 R_3 + \dots + A_n R_n}{A_1 + A_2 + A_3 + \dots + A_n} \quad (1)$$

where \bar{R} denotes the average rainfall and $R_1, R_2, R_3, \dots, R_n$ indicate the rainfall measured at the corresponding rainfall station 1, 2, ..., n , with n defining the number of stations. The contribution of each station into the average of rainfall, \bar{R} , was determined from its corresponding area of polygon, $A_1, A_2, A_3, \dots, A_n$. Analysis of the rainfall frequency employed various distribution types at various return periods. To ensure the most representative probability of the rainfall distribution among the tested distributions, the Smirnov-Kolmogorov method was applied for the goodness-of-fit test.

To evaluate the area of land cover for each land use classification, the QGIS application was utilized. Parameter based on the hydrologic soil group (HSG) was arranged to evaluate the possibility of runoff flow, the curve number, CN , the maximum potential of water retention, S , and the effective rainfall, P_e [12]. This effective rainfall based on the CN values can be quantified as follows:

$$P_e = \frac{(P - 0,2 S)^2}{P + 0,8 S} \quad (2)$$

$$S = \frac{25400}{CN} - 254 \quad (3)$$

Herein, P_e defines the effective rainfall computed in mm while P denotes the rain distribution given in mm. The rainfall intensity was required to compute the rainfall distribution and its duration over 7 hours. Using the Mononobe method, the intensity of rainfall can be expressed as Equation (4) [13].

$$I = \frac{X_{tr}}{24} \left(\frac{24}{t} \right)^{2/3}, \quad (4)$$

where I denotes the design rainfall intensity, X_{tr} the maximum height of daily rainfall and t represents the rain duration or concentration time given in hour. Furthermore, the hyetograph of the design rainfall was arranged using the Alternating Block Method (ABM) and the prediction of the rainfall intensity [12]. Having analysed the aforementioned parameters, the present study predicted the design flood discharge at various return periods of 5-, 10-, 25-, 50- and 100-year using two different methods, namely the HSS SCS [12] and HSS Snyder [14].

3. Result and Discussion

3.1. Analysis of Maximum Rainfall

This study has employed the rainfall data measured from 2012 to 2021 at the Kebun Rambutan, SMPK Marihat, Sei Putih and Gunung Pamela rainfall stations [15]. The Polygon Thiessen representing the Padang watershed and constructed from these four stations is shown in Fig. 1(a). Its location relative to nearby cities

in the Province of North Sumatera, Indonesia is presented in Fig. 1(b). By using the Polygon Thiessen method and the rainfall data, the average of rainfall was analysed and the maximum monthly rainfall, R_{max} , computed from ten consecutive years is presented in Tabel 1.

Table 1. Maximum monthly rainfall, R_{max} (mm).

Year	R_{max} (mm)
2012	107,49
2013	95,06
2014	93,93
2015	126,12
2016	72,02
2017	99,69
2018	71,18
2019	96,55
2020	87,70
2021	84,77

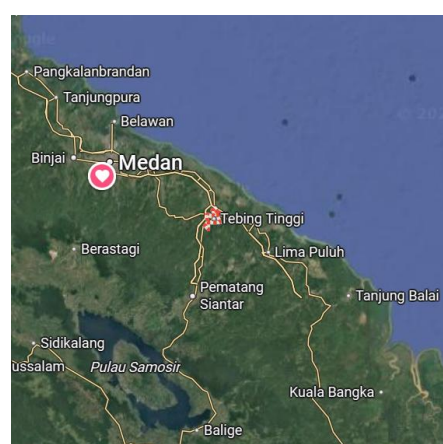
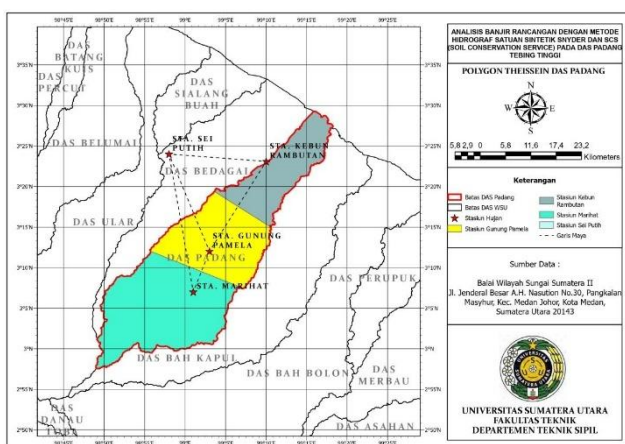


Figure 1. (a) Polygon Thiessen representing Padang watershed and (b) its location relative to other cities in the Province of North Sumatera, Indonesia.

3.2. Analysis of Periodic Rainfall and Representative Distribution

Analysis of periodic rainfall was computed using the distribution of Gumbel, Normal, Log Normal and Log Pearson III. Table 2 outlines the periodic rainfall frequency applied to the watershed for each distribution. It shows that the rainfall increases with the return period regardless of the distribution applied.

Table 2. Periodic rainfall, X_{tr} (mm).

Return Period (year)	Gumbel	Normal	Log Normal	Log Pearson III
5	110,65	107,11	106,61	106,60
10	123,50	114,27	115,03	115,15
25	138,49	121,23	123,87	125,07
50	151,78	126,79	131,40	131,96
100	163,74	131,34	137,91	138,50

In order to determine the most representative distributions, it is deemed necessary to analyze various statistical parameters including the mean rainfall, \bar{X} , standard deviation, S_x , variation coefficient, C_v , skewness coefficient, C_s , and the curtosis coefficient, C_k . The results were then compared with the requirements based

on the distribution type [13]. Table 3 indicates the comparisons of the statistical parameters obtained from the various distributions and hence the most representative distribution. It confirms that the Log Pearson distribution III has fulfilled the fitting condition that requires no specific values of the statistical parameters.

Table 3. Analysis of statistical parameters depending on the distribution type.

Distribution Type	Statistical Parameters	Indications
Gumbel	$C_s = 0,52$	Not fulfilled
	$C_k = 4,66$	Not fulfilled
Normal	$C_s = 0,52$	Not fulfilled
	$C_k = 4,66$	Not fulfilled
Log Normal	$C_s = 0,05$	Not fulfilled
	$C_k = 4,12$	Not fulfilled
Log Pearson Type III	$C_s = 0,05$	Fulfilled
	$C_k = 4,12$	Fulfilled

3.3. Analysis of Kolmogorov-Smirnov Test

The Kolmogorov-Smirnov test was undertaken to evaluate the goodness of fit presented by the Log Pearson III distribution. This evaluation requires ordering from the largest to the smallest value of the maximum monthly rainfall shown earlier in Table 1. The order requires the data presented in logarithmic value, $\log X_i$. Table 4 shows the results of the Kolmogorov-Smirnov test, showing the empirical probability, $P(X_i)$, frequency factor, $f(t)$, theoretical probability, $P'(X_i)$, and the net between the empirical and the theoretical probability, ΔP . This computation results in the standard deviation, S , estimated at 0.08.

Table 4. Parameters arising in the Smirnov-Kolmogorov test.

i	$\log X_i$ (mm)	$P(X_i)$	$f(t)$	$P'(X_i)$	ΔP
1	2,10	0,09	1,81	0,04	-0,06
2	2,03	0,18	0,89	0,19	0,00
3	2,00	0,27	0,45	0,33	0,05
4	1,98	0,36	0,27	0,39	0,03
5	1,98	0,45	0,18	0,43	-0,03
6	1,97	0,55	0,11	0,46	-0,09
7	1,94	0,64	-0,29	0,61	-0,02
8	1,93	0,73	-0,49	0,69	-0,04
9	1,86	0,82	-1,43	0,92	0,11
10	1,85	0,91	-1,50	0,93	0,02
ΔP_{max}					0,11

Table 4 also shows that ΔP_{max} is estimated at 0.11; this being smaller than the acceptable critical value (i.e. $\Delta P_{kritis} = 0,41$ for degree of confidence set at 5% and 10 existing data). Based on this comparison, the distribution of Log Pearson III probability can be accepted to further analyse the rainfall data.

3.3. Analysis of Land Use

The area of land use covering the Padang watershed for each classification of land use is presented in Table 5. The present analysis indicates that the largest area in this study case lies in the classification of dry land agriculture. The land use classification existing in the Padang watershed is qualitatively presented in Fig. 2. Both dry land agriculture and plantation fields dominate the watershed.

Table 5. Land use and land cover area covering the Padang watershed.

Land Use Classification	Area (Ha)

Shrub Forest	4657,99
Swamp Forest	31,54
Secondary Dry Land Forest	7414,00
Secondary Mangrove Forest	382,30
Urban area	2934,46
Plantation	40160,21
Dry Land Agriculture	46930,69
Mixed Dry Land Agriculture	765,26
Paddy Field	5821,85
Fish/Shrimp Farm	418,13
Unused Land	782,48
Water Body	532,09

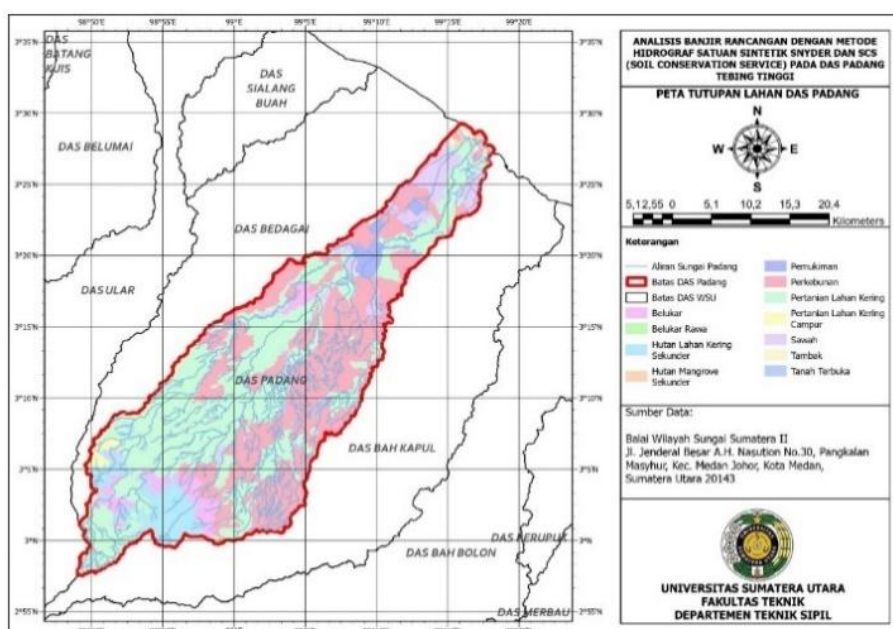


Figure 2. Land cover map of Padang watershed.

3.4. Analysis of Soil Type and CN Number

Analysis of soil type was conducted by following the FAO/UNESCO system that considers Soil Hydrological Group (SHG) [16]. The soil type and code applied for the Padang watershed as well as its corresponding area are presented in Table 6. The map of the soil type is shown in Fig. 3. The dominant soil types existing in the watershed cover Ferric Acrisols, *4f*, Orthic Ferralsols, *Fo*, and Dystric Fluvisols, *Jd*. Based on this soil type data, the classifications of the land use, the SHG and the CN number are computed [17]. Table 7 presents all these classifications along with its quantitative values.

Table 6. Soil code, soil type and SHG existing in the Padang watershed.

Soil Code	Soil Type	SHG	Area (Ha)
Af	<i>Ferric Acrisols</i>	D	16699,24
Fo	<i>Orthic Ferralsols</i>	B	80058,40
Jd	<i>Dystric Fluvisols</i>	C	14073,37

Table 7. SHG, CN and % CN for each land use classification in the Padang watershed.

Land Use Classification	SHG	CN	% CN
Shrub Forest	D	83	38,52
	B	59	220,59
Swamp Forest	C	100	2,85
Secondary Dry Land Forest	B	60	401,37
Secondary Mangrove Forest	C	98	33,80
	D	92	158,09
Urban Area	B	85	8,74
	C	90	74,39
	D	83	680,36
Plantation Field	B	69	1739,65
	C	78	220,44
	D	86	306,96
Dry Land Agriculture	B	75	2613,72
	C	82	321,89
Mixed Dry Land Agriculture	B	71	49,02
	D	85	77,40
Paddy Field	B	73	23,62
	C	81	325,53
Fish/Shrimp Farm	C	100	37,73
	D	83	7,06
Unused Land	B	69	34,79
	C	78	9,11
	D	100	12,29
Water Body	B	100	12,37
	C	100	6,84
	C	100	16,51
% Total			74,33

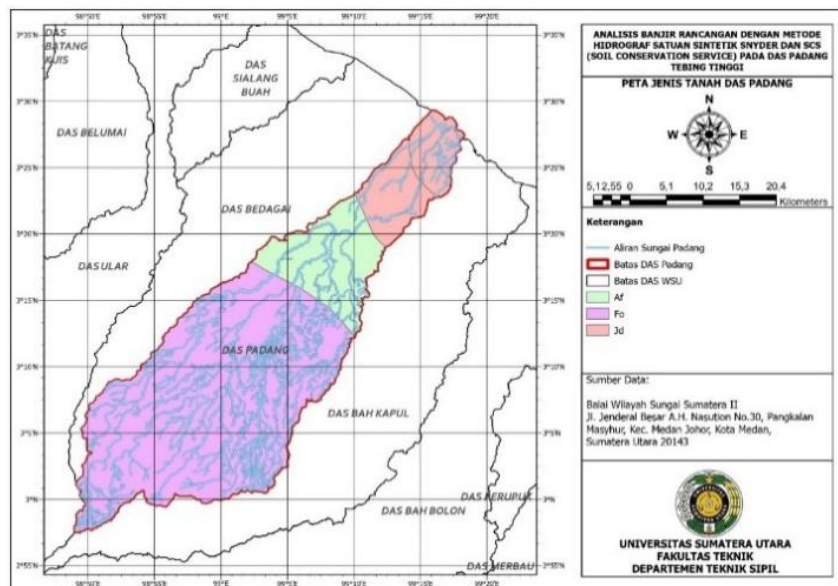


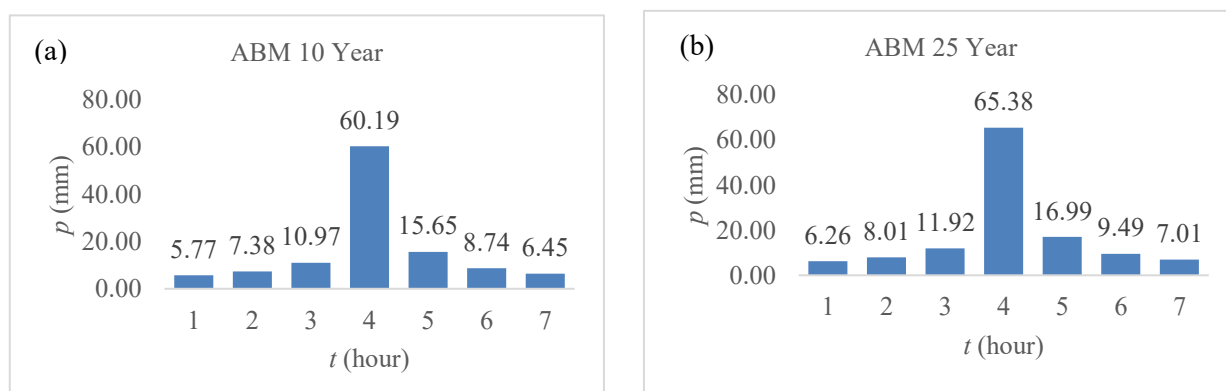
Figure 3. Soil type distribution covering Padang watershed.

3.5. Analysis of Rainfall Intensity and Hourly Rainfall Distribution

The intensity of the rainfall was evaluated using the Mononobe method with the time duration set over 7 hours [18]. The computations for various time durations and return periods are given in Table 8. Furthermore, using these rainfall intensity data, the hourly rainfall distributions predicted at the return period of 10-, 25-, 50- and 100-year are given in hyetograph (see Fig. 4). This distribution was computed by employing the ABM method. It shows the rainfall intensity associated with each rain duration. Similar trends showing peak rain distribution at the fourth hour are observed across various return periods.

Table 8. Rainfall intensity, I , analysed with variations in duration and return period.

Return Period (year)	Rainfall Intensity, I (mm/jam)						
	1	2	3	4	5	6	7
5	36,96	23,28	17,77	14,67	12,64	11,19	10,10
10	39,92	25,15	19,19	15,84	13,65	12,09	10,91
25	43,36	27,31	20,84	17,21	14,83	13,13	11,85
50	45,75	28,82	21,99	18,15	15,65	13,85	12,50
100	48,02	30,25	23,08	19,06	16,42	14,54	13,12



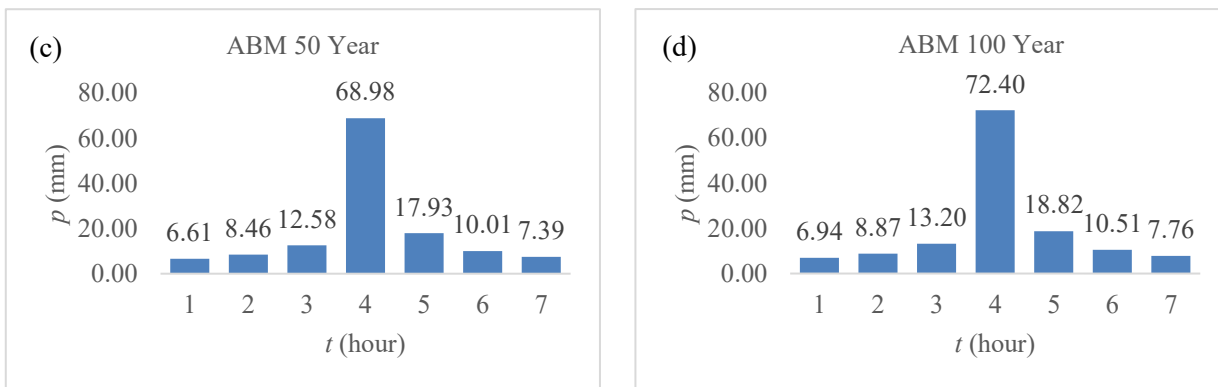


Figure 4. Hyetograph of rain distribution, p , based on the ABM method in cases of various return periods.

3.6 Analysis of Effective Rainfall

The next investigation concerns the effective rainfall, p_e , and the depth of rain accumulated over the required time duration, p_{cum} . The effective rainfall was computed using the formula valid for the condition where $p_{cum} \geq 0.2 S$ [13]. The present study has applied $0.2S = 17.54$ mm, such that for the precipitation being smaller than 17.54 mm, infiltration is considered and hence no flow running on the ground surface is assumed. Given this consideration, each condition of $p_{cum} < 17.54$ results in the case of $p_e = 0$. Table 9 outlines the effective rainfall for each return period of 5-, 10-, 25-, 50- and 100-year. These p_e values were then adopted as the design rainfall for determining the hydrograph in the analysis of design flood discharge [13].

Tabel 9. Effective rainfall, p_e , for various return periods.

T (tahun)	t (jam)	p_{cum} (mm)	p_e (mm)	Δp_e (mm)
5	1	5,34	0,00	0,00
	2	12,17	0,00	0,00
	3	22,33	0,25	0,25
	4	78,06	24,71	24,46
	5	92,54	34,58	9,87
	6	100,63	40,43	5,85
	7	106,60	44,88	4,45
10	1	5,77	0,00	0,00
	2	13,15	0,00	0,00
	3	24,12	0,46	0,46
	4	84,31	28,87	28,41
	5	99,96	39,93	11,07
	6	108,70	46,46	6,53
	7	115,15	51,41	4,95
25	1	6,26	0,00	0,00
	2	14,28	0,00	0,00
	3	26,20	0,78	0,78
	4	91,58	33,89	33,12
	5	108,57	46,37	12,47
	6	118,06	53,69	7,32
	7	125,07	59,23	5,54
50	1	6,61	0,00	0,00
	2	15,06	0,00	0,00
	3	27,64	1,04	1,04
	4	96,62	37,50	36,46

	5	114,55	50,96	13,45
	6	124,57	58,83	7,87
	7	131,96	64,77	5,95
	1	6,94	0,00	0,00
	2	15,81	0,00	0,00
	3	29,01	1,33	1,33
100	4	101,42	41,01	39,68
	5	120,23	55,39	14,39
	6	130,74	63,79	8,40
	7	138,50	70,13	6,33

3.7 Analysis of Design Flood Discharge

Two methods were employed for the analysis of design flood discharge, and both require data of catchment area and length of main river. These two parameters are estimated at $1108,31 \text{ km}^2$ and $60,52 \text{ km}$, respectively. The other important parameters associated with the SUH Snyder method can be seen from Table 10. It is noteworthy that the slope coefficient, C_t , and the storage capacity coefficient, C_p , were empirically derived from the topographical condition of the Appalachian highlands in the United States. It may be necessary to adjust the coefficient values for the present study. To confirm this, the hydrograph predicted using the SUH Snyder is given in Fig. 5. It shows that the flood discharge varies with time and reaches its peak value at a certain peak time.

Table 10. Parameters employed in the SUH Snyder method.

Parameter	Value	Unit
Distance between the weight point of catchment area and outlet, L_c	45	km
Slope coefficient, C_t	1,20	-
Storage capacity coefficient, C_p	0,58	-
Effective rainfall duration, t_e	2,34	hour
Chosen time given that $t_e > t_R, t'_p$	13,23	hour
Peak discharge, q_p	13,01	$\text{m}^3/\text{s}/\text{mm}$

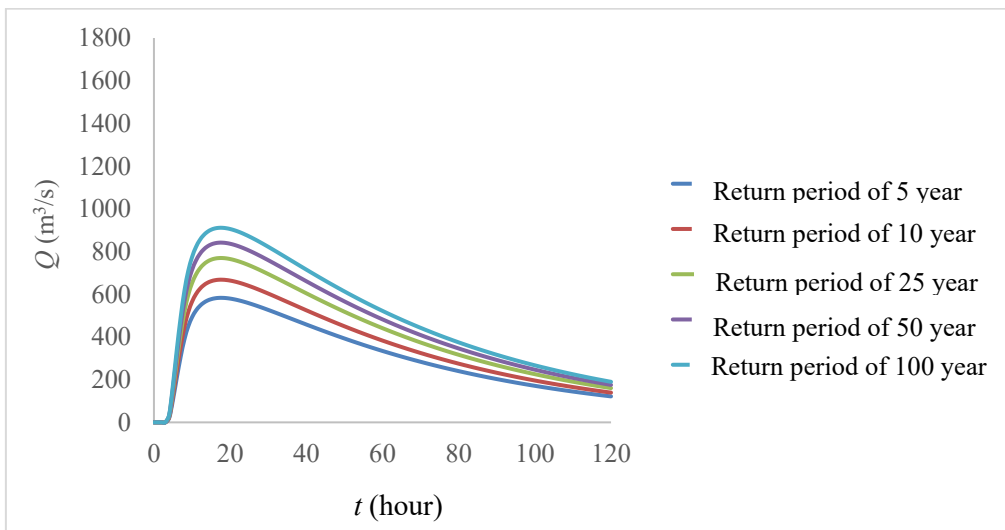


Figure 5. Hydrograph curve predicted by SUH Snyder method.

Based on Fig. 5, the SUH Snyder method estimates that the peak time, T_p , and the peak discharge, Q_p , are respectively 18th hour and 583,10 m³/s in the case of 5-year return period. Interestingly, the peak time appears to vary insignificantly with the return period. In contrast, the peak discharge varies remarkably. The Q_p values are estimated at 668,04 m³/s, 769,53 m³/s, 841,59 m³/s and 911,11 m³/s for the return period of 10-, 25-, 50- and 100-year. Following on, the hydrograph was predicted using the SUH SCS method. The parameters required for this method and the corresponding values are presented in Table 11. Given these parameter values, the hydrograph was observed from Fig. 6. It shows that the peak time, T_p , is estimated at the 10th hour. The corresponding peak discharge, Q_p , is predicted to be 1187,31 m³/s at the return period of 5-year. For cases with higher return periods, the Q_p values increase.

Table 11. Parameters employed in the SUH SCS method.

Parameter	Value	Unit
Concentration time, t_c	14,10	Hour
Delay time, t_p	8,46	Hour
Peak discharge, q_p	23,22	m ³ /s/mm
Baseflow discharge, q_b	11,61	m ³ /s

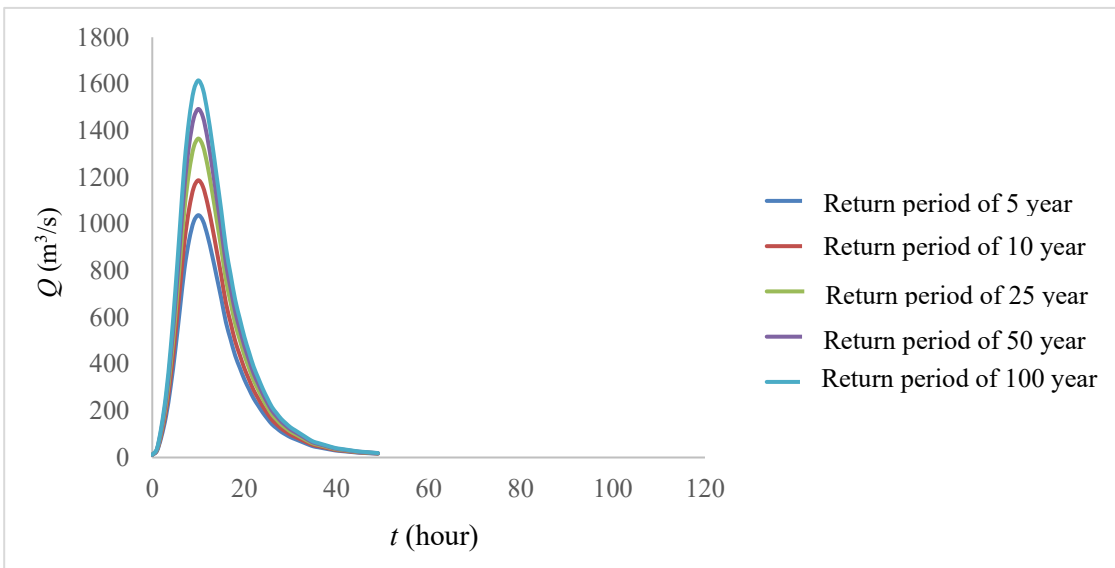


Figure 6. Hydrograph curve predicted by SUH SCS method.

Both methods show similar trends of peak time and peak discharge with the return period. Interestingly, the prediction of peak discharge, Q_p , based on the SUH SCS method are notably larger than the earlier ones given by the SUH Snyder method (see Table 12). The opposite applies for the prediction of peak value, T_p . This value for the SCS method being estimated at 10th hour; this being eight hours earlier than the prediction by the Snyder method. Comparing the computations using the two methods indicates that the ratio of peak discharge is approaching two, particularly at smaller return periods; this being quite a significant deviation (see Fig. 7). Such a discrepancy might be associated with the empirical coefficients, C_t and C_p , being only suitable for certain topography conditions. This relates to the insight that these two coefficients used in the Snyder method, were originally derived from the Appalachian highlands in the United States. Indeed, a similar finding is noted by Siswoyo [7] who predicted the discharge value for the East Java watershed; the discharge value computed

using the SUH Snyder for the watershed of East Java was smaller than computations based on other methods. Moreover, Nugroho [19] who investigated the Ciliwung Hulu watershed, has noted that the SUH SCS would generally predict higher predicted value of peak discharge if compared with measurements. The lower prediction of the peak discharge by the SUH Snyder is due to its longer receding time characterised by less steep hydrograph curve and the requirement to maintain comparable total discharge for both SUH methods. The comparisons observed from the present study further emphasizes the necessity for determining suitable empirical coefficients for the watershed under investigation. Unfortunately, validation of the accurate values of C_t and C_p would require comparison to actual local measurements such as time series of flow discharge. This is left for future studies as different topographical condition would generate different empirical coefficient values.

Table 12. Peak discharge, Q_p , and peak time, T_p , predicted by different methods.

Metode	T	T_p	Q_t	Q_p
	tahun	jam	$m^3/s/mm$	m^3/s
SUH Snyder	5	18	12,79	583,10
	10	18	12,79	668,04
	25	18	12,79	769,53
	50	18	12,79	841,59
	100	18	12,79	911,11
	5	10	22,87	1037,80
SUH SCS	10	10	22,87	1187,31
	25	10	22,87	1365,95
	50	10	22,87	1492,80
	100	10	22,87	1615,17

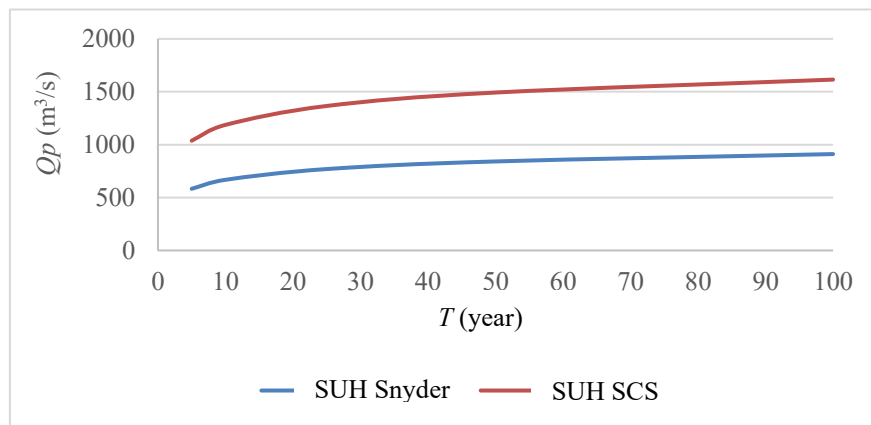


Figure 7. Variation of peak discharge, Q_p , with return period, T , predicted by different methods.

The different values of peak discharge and peak period predicted using the two methods affect the potential risk of flooding in nearby communities. The prediction of the smaller Q_p value by the SUH Snyder method indicates smaller levels of inundation at the riverbank and nearby subdistricts; this suggesting smaller affected areas in total. In contrast, the SUH SCS method not only predicts higher levels of inundation but also a shorter

time duration for the local communities to evacuate prior to the arrival of peak discharge event. Nevertheless, the time duration over which the flooding recedes takes a longer one in the case of Snyder method. This might impact the agility of the local people to recover during a post-flooding phase. Further detailed quantitative studies about the potential risks should be undertaken to get in-depth understanding.

4. Conclusion

The present study has confirmed that the prediction of the design flood discharge by the SUH Snyder method generates smaller values if compared to the estimation by the SUH SCS method. This contrasts with the comparison of the peak time. The deviation between the predictions using these two different methods relates to the empirical coefficients of slope and storage capacity employed in the SUH Snyder. The present study thus highlights the importance of adjusting these two coefficients for the watershed area under investigation. This might be undertaken by considering the proportion of land use existing in the total area of watershed and finding its equivalent coefficient values. Alternatively, one might tune these coefficients such that measurement of the hydrograph curve and its prediction by the Snyder method would provide a good comparison.

In this study, the ratio of the estimation by the two different methods is approaching two, particularly at smaller return periods. For the case of 5-year return period, the SUH Snyder method estimates the peak time at the 18th hour and the peak discharge at 583,10 m³/s. The SUH SCS predicts that the peak time and peak discharge are the 10th hour and 1037,80 m³/s, respectively. Furthermore, this study has indicated the dependence of the peak time and the peak discharge on return period. The former insignificantly varies yet the latter shows a notable variation with the return period. This suggests a careful consideration of return period when designing a flood-control structure. Importantly, when a conservative design is sought out, the SUH SCS is more preferably employed by engineers and local authorities to predict the flooding characteristics. This is supported by its larger prediction of peak discharge and its smaller estimation of peak time, hence requiring a higher elevation and capacity of the structure to withstand the flood.

5. Acknowledgements

The authors would like to thank the support received from Balai Wilayah Sungai (BWS) Sumatera and the constructive feedback from anonymous reviewers.

6. Conflict of Interest

The authors declare that there are no conflicts of interest related to the research, analysis, or publication of this article. All results and interpretations presented in this paper are the outcome of independent and objective scientific investigation.

References

- [1] T. S. Glickman, *Glossary of Meteorology*. 2000.
- [2] N. Purba, "Strategi Mitigasi Penanggulangan Bencana Banjir di Kota Tebing Tinggi Provinsi Sumatera Utara (Studi pada Badan Penanggulangan Bencana Daerah Kota Tebing Tinggi)," *Transformasi: Jurnal Manajemen Pemerintahan*, 2022.
- [3] Pemerintah Kota Tebing Tinggi. (2025, 30 November). Update Laporan Rekapitulasi Data Wilayah Terdampak Banjir Tebing Tinggi. Accessed on 7 Desember 2025, <https://www.tebingtinggikota.go.id/berita/berita-daerah/update-laporan-rekapitulasi-data-wilayah-terdampak-banjir-tebing-tinggi-nov-2025>
- [4] N. F. Margini, D. A. D. Nusantara, dan M. B. Ansori, "Analisa Hidrograf Satuan Sintetik Nakayasu dan ITB Pada Sub DAS Konto, Jawa Timur," *Jurnal Teknik Hidroteknik*, vol. 2, no. 1, hlm. 41-45, 2017.
- [5] L. M. Limantara, *Rekayasa Hidrologi: Edisi Revisi*. Yogyakarta: ANDI, 2018.
- [6] A. Kahfii dan S. Lipu, "Analisis Hidrograf DAS Poso dengan Metode Hidrograf Satuan Sintetis Snyder dan Hidrograf Satuan Sintetis Soil Conversation Service (SCS)," *Rekonstruksi Tadulako: Civil Engineering Journal on Research and Development*, vol. 2, no. 2, hlm. 121-128, 2021.

- [7] H. Siswoyo, "Pengembangan Model Hidrograf Satuan Sintetis Snyder untuk Daerah Aliran Sungai di Jawa Timur," *Jurnal Teknik Pengairan: Journal of Water Resources Engineering*, vol. 2, no. 1, hlm. 42-54, 2011.
- [8] A. N. Sari, R. Pranoto, dan V. Suryan, "Perhitungan Hidrograf Banjir dengan Metode Hidrograf Satuan Sintesis SCS (Soil Conservation Service) di Kota Palembang," *Journal of Airport Engineering Technology (JAET)*, vol. 1, no. 1, hlm. 1-7, 2020.
- [9] Z. Erwanto dan B. Baried, "Studi Optimasi Penggunaan Lahan dalam Pengelolaan DAS Tambong Banyuwangi Berdasarkan HSS US SCS," *Logic: Jurnal Rancang Bangun dan Teknologi*, vol. 14, no. 1, hlm. 22-27, 2014.
- [10] F. P. Siregar, "Analisis Pengendalian Debit Banjir Sungai Padang di Kota Tebing Tinggi," *Laporan Tugas Akhir Universitas Medan Area*, 2017.
- [11] Balai Wilayah Sungai Sumatera II, "Data Geografis DAS Padang," Medan, 2023.
- [12] S. Salsabila, "Analisis Pengaruh Perubahan Tata Guna Lahan terhadap Debit Banjir DAS Deli dengan Metode HSS SCS -CN," 2021.
- [13] I. M. Kamiana, *Teknik Perhitungan Debit Rencana Bangunan Air*. Yogyakarta: Graha Ilmu, 2011.
- [14] F. A. Siahaan, "Analisis Banjir Rancangan dengan Metode Hidrograf Satuan Sintetik Snyder dan SCS (Soil Conservation Services) DAS Deli (Studi Kasus)," 2018.
- [15] Stasiun Klimatologi Kelas I Sampali, "Data Curah Hujan," Deli Serdang, 2023.
- [16] D. S. Subardja, S. Ritung, M. Anda, E. Suryani, dan R. E. Subandiono, *Petunjuk Teknis Klasifikasi Tanah Nasional*, 1 ed. Bogor: Balai Besar Litbang Sumberdaya Lahan Pertanian, Badan Penelitian dan Pengembangan Pertanian, 2014.
- [17] Arsyad Sitanala, *Konservasi Tanah & Air*, 2 ed. Bogor: IPB PRESS, 2010.
- [18] K. Christian, D. Yudianto, dan S. R. Rusli, "Analisis Pola Distribusi Hujan Terhadap Perhitungan Debit Banjir DAS Cikapundung Hulu," *Jurnal Teknik Sumber Daya Air*, vol. 3, no. 3, hlm. 153-160, 2017.
- [19] S. P. Nugroho, "Analisis Hidrograf Satuan Sintetik Metode Snyder, Clark dan SCS dengan menggunakan Model HEC-1 di DAS Ciliwung Hulu," *Jurnal Sains & Teknologi Modifikasi Cuaca*, vol. 2, no. 1, hlm. 57-97, 2001.